Solar Energy Materials & Solar Cells 166 (2017) 132–139

Contents lists available at ScienceDirect

Solar Energy Materials & Solar Cells

journal homepage: www.elsevier.com/locate/solmat

Influence of surface structure of n-type single-crystalline Si solar cells on potential-induced degradation

Kohjiro Hara[a,*], Kinichi Ogawa[a], Yusuke Okabayashi[b], Hiroyuki Matsuzaki[b], Atsushi Masuda[a]

[a] Research Center for Photovoltaics, National Institute of Advanced Industrial Science and Technology (AIST), 807-1 Shuku-machi, Tosu, Saga 841-0052, Japan

[b] Research Institute for Measurement and Analytical Instrumentation, AIST, 1-1-1 Umezono, Tsukuba, Ibaraki 305-8568, Japan

ARTICLE INFO

Keywords:
Potential-induced degradation (PID)
N-type crystalline Si solar cell
Photovoltaic module
Surface polarization
Front surface recombination
Passivation

ABSTRACT

Potential-induced degradation (PID) in photovoltaic (PV) modules based on n-type single-crystalline Si solar cells (a bifacial cell, interdigitated back contact cells, and a hetero junction (HJ) cell) was experimentally investigated by applying high voltages to the modules. The power output of a PV module with an n-type bifacial-front junction (FJ) Si solar cell decreased by about 17% by applying −1000 V at 85 °C for 10 min, whereas no degradation was observed by applying +1000 V at 85 °C for 10 min. The spectrum of external quantum efficiency and transient absorption kinetics of the module after PID tests indicated that surface charge recombination between electron and hole on the Si cell was enhanced. PID in n-type Si PV modules can be approximately explained by surface polarization enhancing front surface recombination on Si cells, which corresponds to a loss of passivation effect by a silicon nitride (SiN_x) layer. On the other hand, no PID was observed in a PV module with an n-type bifacial-rear junction (RJ) Si solar cell and a commercial PV module based on an HJ cell by applying both positive and negative voltages. High conductive layers of transparent conductive oxide (TCO) on the top of HJ Si solar cells would significantly effective to suppress PID in n-type Si PV modules.

1. Introduction

Potential-induced degradation (PID) in crystalline Si photovoltaic (PV) modules was observed in PV systems where many PV modules are serially interconnected, resulting in significant power losses in the system. PID has been typically investigated in Si PV modules with p-type-based crystalline Si solar cells [1–23]. The factor causing PID is considered to be sodium ion (Na^+), which is involved in a soda lime front cover glass [2–4,18–23], and other ions or charges [5–7]. In addition, Naumann and co-workers have proposed that PID is caused by Na-decorated stacking faults in Si solar cells [12–15], and Na^+ originates from a contamination on the surface (e.g. SiN_x layer) [14,15]. Decrease in the shunt resistance of modules owing to the influence of ions, such as Na^+, on the p-n junction of Si cells would be main reason leading to PID in p-type Si PV modules [1,4,5,10,14].

In contrast, detail studies on PID in PV modules based on n-type crystalline Si solar cells have been less than p-type Si PV modules, and have been typically investigated by using interdigitated back contact (BC) Si solar cells, since SunPower firstly reported in 2005 [24]. Swanson et al. reported that the PV performance of a high-efficiency n-type BC Si PV module decreased by applying high positive voltage to the Si cell by surface polarization effect [24]. By the polarization effect, negative charges are left on the front surface of the n-type Si cell, enhancing front surface recombination between electrons and holes at the surface [24].

Naumann et al. also reported PID in an n-type BC solar cell [25]. In their study, however, degradation occurred by applying negative voltage from the ground toward the Si cell [25]. In addition, Halm et al. reported that PID in an n-type BC solar cell with a p^+ front floating emitter occurred by applying negative high voltage stress to the Si cell [26]. They concluded that the power drop of the module is related to the degradation of front surface passivation enhancing surface charge recombination [26], as reported by Swanson et al. [24]. Thus, PID in PV modules based on n-type BC Si solar cells can be basically explained by degradation of surface passivation enhancing surface charge recombination, whereas the voltage polarity causing PID might depend on the type of surface layer (n or p) of BC Si solar cells.

We have reported that PID occurred in PV modules based on an n-type front junction Si solar cell (not BC cell) by applying negative voltage stress to the Si cell, whereas no degradation was observed by

* Corresponding author.
E-mail address: k-hara@aist.go.jp (K. Hara).

http://dx.doi.org/10.1016/j.solmat.2017.03.018
Received 11 July 2016; Received in revised form 28 December 2016; Accepted 16 March 2017
Available online 23 March 2017

applying positive voltage [27]. The external quantum efficiency (EQE) in the range from 400 to 600 nm significantly decreased after negative voltages were applied, although no change was observed in the range from 800 to 1100 nm [27]. This suggested that front surface charge recombination was enhanced by PID, as reported in n-type BC Si PV modules [24–26]. Because n-type Si PV modules have attracted attention owing to their high efficiency, detail mechanism of PID in not only n-type BC Si PV modules, but also other n-type Si PV modules should be investigated furthermore.

In this paper, we focus on influence of the surface structure of n-type-based bifacial Si solar cell in terms of the position of junction (front or rear side) and the condition of a surface layer of silicon nitride (Si_3N_4 or SiN_x) for anti-reflection (AR) coating and passivation on PID to understand PID in n-type Si PV modules furthermore. In addition, PID in commercial full-size n-type Si PV modules based on a hetero junction (HJ) and BC Si solar cells was also experimentally investigated. Influence of the surface structure of n-type-based Si solar cells on PID and technique for suppression of PID in n-type Si PV modules are shown and discussed.

2. Experimental

2.1. Module fabrication of single-cell module

Schematic structures of n-type-based single-crystalline Si solar cells used in this study are shown in Fig. 1. A commercial n-type-based bifacial Si solar cell (size is 156 mm×156 mm, ca. 200-μm thickness) was employed. We used the Si cells whose p-layer is on the front side (front junction, FJ, as shown in Fig. 1a) and that is on the rear side (rear junction, RJ, Fig. 1b). We also employed an FJ Si solar cell whose refractive index (RI) of the AR coating composed of SiN_x and SiO_x layers was changed to 2.34 (i.e. Si rich condition); the RI for the standard Si cell is 2.05. Additionally, an FJ Si solar cell without the layer of SiN_x (there is only the SiO_x layer) was employed to investigate influence of the surface structure of Si solar cells on PID. A commercial p-type multi-crystalline Si solar cell (size is 156 mm×156 mm, ca. 200-μm thickness) was also used for single-cell module as a reference.

The standard Si PV module (single-cell module) consisted of a front cover glass (Asahi Glass Co., Ltd., strengthen soda lime glass, 3.2-mm thickness, 180 mm×180 mm), two films of commercial EVA (fast-cure-type, 0.45-mm thickness) as encapsulant, a Si solar cell, and a commercial back sheet whose structure is polyvinyl fluoride (PVF)/polyethylene terephthalate (PET)/PVF. The PV module components (glass/EVA/c-Si cell/EVA/back sheet) were laminated by using a laminator (LM-50×50, NPC Inc.) under vacuum condition at 150 °C for 20 min. Two types of module were fabricated by changing the front and rear sides of the bifacial Si cell for the top (glass side); the p-n junction is located at the front side (FJ-type) and the back sheet side (RJ-type).

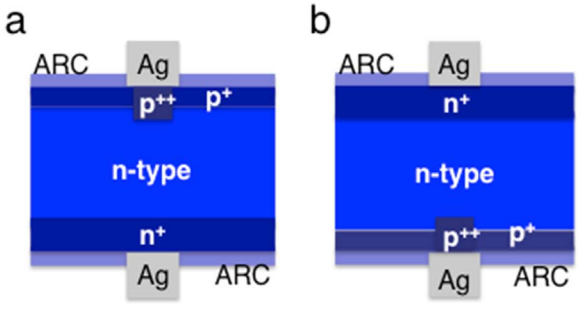

Fig. 1. Schematic structures of n-type-based bifacial-crystalline Si solar cells; (a) a front junction (FJ) cell and (b) a rear junction (RJ) cell (ARC is anti-reflection coating).

2.2. Full-size commercial modules

The PID-resistant property of full-size commercial n-type Si PV modules was also investigated. Three commercial modules, module A based on an HJ Si solar cell, modules B and C with interdigitated BC Si solar cells whose PV supplier are different, were employed for PID tests.

2.3. PID tests for single-cell module and commercial modules

In order to homogeneously apply voltage to Si cells, an Al plate (ca. 0.5-mm thickness) was strictly attached on the entire front cover glass of single-cell modules as the electrode for PID tests, as reported in previous papers [21–23,27]. Negative or positive high voltage was applied to Si cells with respect to the Al plate by using a power supply (Kikusui Electronics Corp., TOS7200) at 60 °C or 85 °C in a chamber; e.g. −100 V at 60 °C for 1 h, −1000 V at 85 °C for 10 min or 2 h. The humidity in the chamber was not controlled during PID tests (ca. 2% at 85 °C). The PID test for commercial modules was firstly conducted by applying positive voltage (+1000 V) to Si cells (string) with respect to the Al frame of modules at 85 °C with relative humidity of 85% for 96 h in an environmental chamber, and then the performance of the module was measured. Next, negative voltage (−600 V or −1000 V) was applied from the Al frame to the Si cell at 85 °C with 85% for 96 h as the secondary PID test.

2.4. Characterization of PV modules

Solar energy-to-electricity conversion efficiency (η) of Si PV modules before and after the PID tests was measured by using I-V curve measurement systems with an AM 1.5 G solar simulator with a Xe lamp as the light source (Yamashita Denso Corp., YSS-150A for single-cell modules, and Nisshinbo Mechatronics Inc., PVS1222i for full-size commercial modules). Electroluminescence (EL) images of PV modules were measured by using an EL measurement system (ITES Co., Ltd.) equipped with a digital camera and a DC power supply (Kikusui, PWR1600M). A similar system equipped with a digital camera and an LED light source (ITES) was employed for the measurement of photoluminescence (PL) images of PV modules before and after the PID tests (the excitation wavelength is 850 nm).

Spectra of external quantum efficiency (EQE) for the modules were estimated with a spectral photocurrent response measurement system (Bunkoukeiki Co., Ltd., BQE-100L). The EQE was measured using PV modules through glass and encapsulant, because we do not use adhesive to fix the Al plate on the glass of modules during PID tests. Therefore, we can avoid influence of residues, which affects the glass transmittance.

2.5. Time-resolved diffuse reflectance measurement

Time-resolved diffuse reflectance spectroscopy (TR-DRS), where diffuse-reflected light is used as probe light instead of transmitted light, is a powerful method to analyze the dynamics of photo-excited states in optically opaque systems [28,29]. In the TR-DRS, transient absorption intensity can be expressed as %absorption (%Abs) given by $\%Abs=100\times(1-R/R_0)$, where R and R_0 represent the intensity of probe diffuse-reflected light with and without pump-light excitation, respectively.

TR-DRS measurements were carried out with a Nd:YAG laser (SL311, Ekspla, wavelength of 1064 nm, pulse width of 150 ps, and repetition rate of 10 Hz) and Ti: Al_2O_3 regenerative amplifier (Solstice, Spectra Physics, wavelength of 800 nm, pulse width of 100 fs, repetition rate of 1 kHz). For 532-nm and 1064-nm excitation, the second harmonic light (532 nm) and fundamental light (1064 nm) of Nd: YAG laser were used. For 400-nm excitation, the second-harmonic light (400 nm) generated from fundamental light (800 nm) of Ti: Al_2O_3

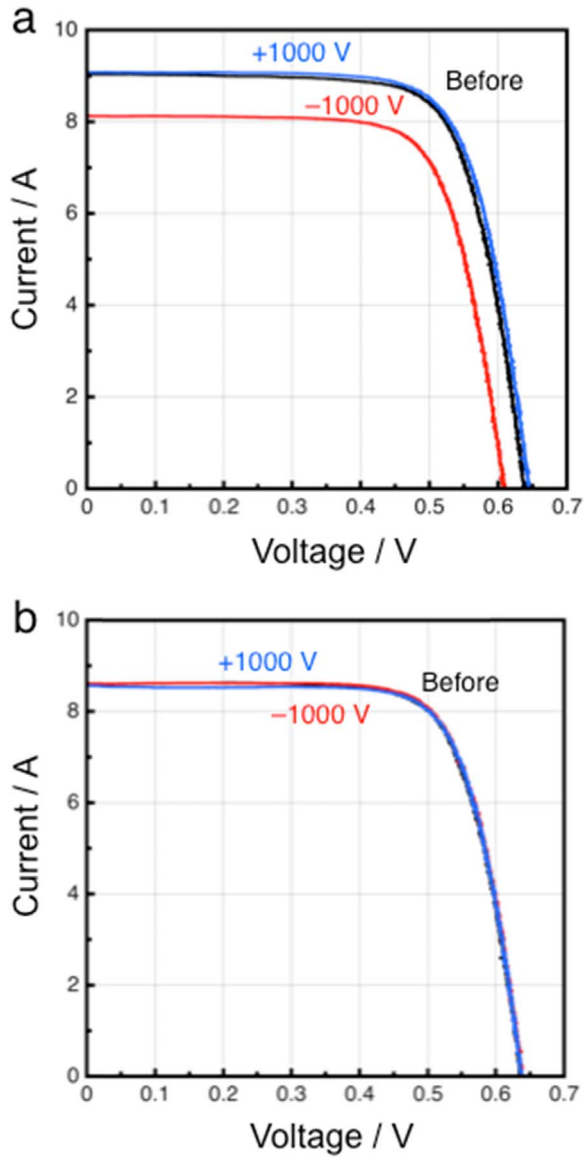

Fig. 2. I-V curves for the standard PV module based on n-type single-crystalline Si PV modules (a) bifacial FJ and (b) bifacial RJ before and after PID tests; (black) before, (red) −1000 V at 85 °C for 10 min, and (blue) +1000 V at 85 °C for 10 min, respectively. (For interpretation of the references to color in this figure legend, the reader is referred to the web version of this article.)

regenerative amplifier was used. A steady-state cw Xe arc lamp (UXL-75XE, USHIO Inc., 75 W) was used as the probe light source. The pump and probe lights were focused on sample with ~12 mm and ~6 mm in diameter. The diffuse-reflected probe light from the sample was detected using an InGaAs photodetector (DET20C, Thorlabs) after being broadly monochromatized (1500–1800 nm range) with an optical filter. At this wavelength range of probe light below the bandgap of Si, photo-induced signal due to photo-generated carriers in Si can be detected. The AC signal from the photodetector were amplified with a voltage amplifier (DHPVA-100, Femto), and then processed and analyzed with a digital oscilloscope (Waverunner6200A, LeCroy). The DC offset signal from the detector was subtracted separately and the monitored using a multimeter. As a result, small signals of % Abs (< 0.2) were detected with 40-ns time resolution.

3. Results and discussion

3.1. PID in the standard module (bifacial Si cell)

Fig. 2 shows I-V curves for the standard n-type (a) FJ and (b) RJ Si PV modules before and after PID tests by applying −1000 V at 85 °C for 10 min and +1000 V at 85 °C for 10 min, respectively. The η of the FJ Si PV module decreased from 17.5% to 14.6% after the PID test of −1000 V at 85 °C for 10 min (the power output decreased by about 17%), as shown in Fig. 2a. Both short-circuit current (I_{sc}) and open-circuit voltage (V_{oc}) decreased from 9.05 A to 8.12 A and from 0.64 to 0.60 V, respectively, although fill factor was not changed as 0.72. The decreased performance was completely recovered after applying +1000 V at 85 °C for 10 min (Fig. 2a). These results obviously indicate that negative voltage to the Si cell with respect to the Al plate is an important factor causing PID in the n-type FJ Si PV module used in this study, and the degradation is completely reversible.

Similar degradation in the standard FJ Si PV module was also observed by applying −100 V at 60 °C for 1 h (the η decreased from 17.5% to 15.0%), whereas PID did not occur in the p-type multi-crystalline Si PV module by the same PID test (data are not shown). It should be noted that PID occurs in n-type FJ Si PV module by a voltage stress condition, which did not cause PID in p-type Si PV modules. These results imply that the mechanism of PID in the n-type FJ Si PV module is different from that in p-type Si PV modules. Generally, metal ions, such as Na^+, are considered to be the essential factor causing PID in p-type Si PV modules [12–23], as mentioned in Introduction. It is possible that metal ions, such as Na^+, which originate from soda lime glass or contamination, are not related to PID in the n-type FJ Si PV module. On the other hand, Halm et al. proposed that contamination of the emitter by mobile ions influences PID in an n-type BC solar cell by PID [26]. Mechanisms of PID in n-type Si PV modules are shown and discussed in Section 3.5.

Fig. 3 shows EL and PL images for the n-type FJ Si PV module before and after the PID tests (−1000 V at 85 °C for 10 min and +1000 V at 85 °C for 10 min, respectively). After PID occurred by applying −1000 V, the entire Si cell was homogeneously darkened, whereas the EL-inactive darkened areas were partially observed in p-type Si PV modules [1,8,16,21–23]. This change in the EL images after the PID test also suggests different degradation mechanism between n-type and p-type Si PV modules. After applying +1000 V at 85 °C for 10 min, the EL and PL images were completely recovered, as shown in Fig. 3.

In contrast to the FJ Si PV module, no degradation was observed in the RJ Si PV module after PID tests by applying −1000 V at 85 °C for 10 min and +1000 V at 85 °C for 10 min, respectively (Fig. 2b). These results suggest that surface polarization does not occur in the n-type RJ

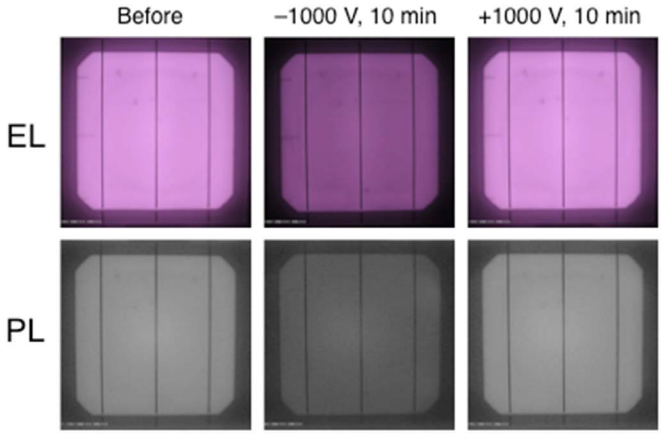

Fig. 3. EL and PL images for the standard n-type FJ Si PV module before and after PID tests (−1000 V at 85 °C for 10 min and +1000 V at 85 °C for 10 min).

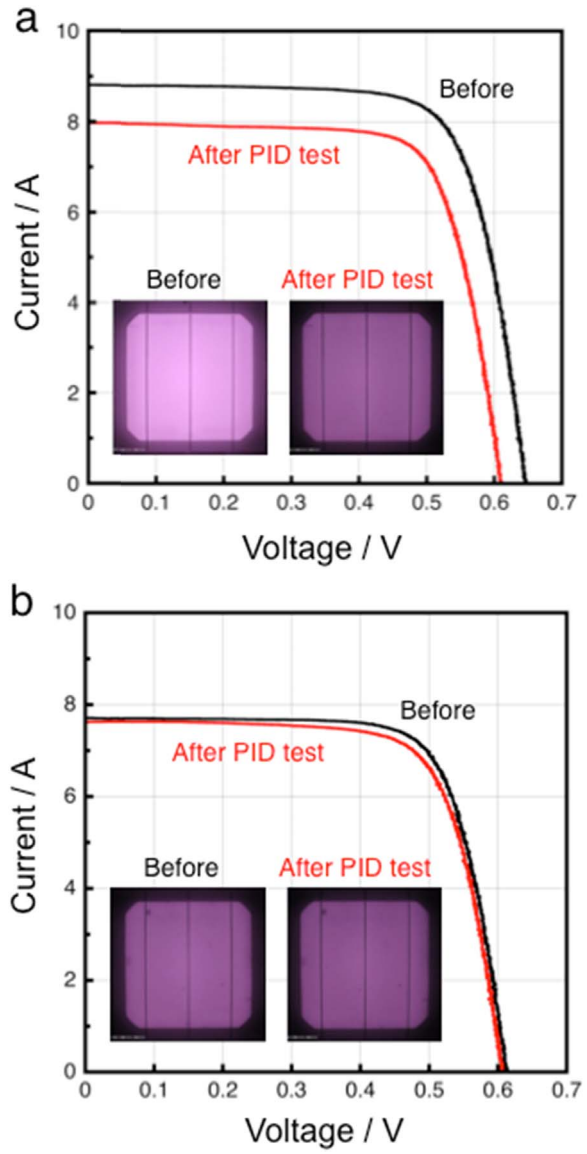

Fig. 4. I-V curves and EL images for an n-type bifacial FJ Si PV modules before and after PID test by applying −100 V at 60 °C for 1 h; (a) whose RI of the SiN_x layer was changed from 2.05 to 2.34 (i.e. Si rich condition) and (b) without SiN_x layer.

Si module used in this study. A high PID-resistivity of an n-type rear-emitter Si PV solar cell was also reported by Yamaguchi et al. [30]. On the other hand, Pingel et al. reported that degradation was observed in PV modules based on n-type bifacial back side Si solar cell, which corresponds to a RJ cell, by applying both −1000 V and +1000 V [31]. They mentioned that both passivated front and rear sides were affected by PID in the case of bifacial Si solar cells. These different behaviors would be attributed to the different surface structure (e.g. AR and passivation layers) of Si cells, whereas the detail is unclear.

3.2. Influence of SiN_x layer on PID

We have investigated influence of the surface structure of AR and passivation layers on PID in n-type Si PV modules furthermore. Fig. 4a shows I-V curves and EL images for an n-type PV module based on an FJ Si cell whose RI of the SiN_x layer was changed from 2.05 to 2.34 (i.e. Si rich condition), before and after PID tests by applying −100 V at 60 °C for 1 h. The η of the module decreased from 17.5% to 15.0% after the PID test by applying −100 V at 60 °C for 1 h, which is similar to the degradation observed in the module based on the standard Si cell. It has been reported that PID can be significantly suppressed by increasing the RI of SiN_x layers as AR coating on the surface of p-type crystalline Si solar cells [1,6,19,20]. Our result indicates that a control of the RI for SiN_x is not effective to prevent surface polarization causing PID in n-type Si PV modules.

I-V curves and EL images for a Si PV module based on an n-type FJ Si cell without a layer of SiN_x (with only a SiO_x layer), which is for both AR coating and passivation, before and after PID tests by applying −100 V at 60 °C for 1 h are shown in Fig. 4b. Before the PID test, the I_{sc} decreased from 9.05 A (Fig. 2a) for the standard module including a SiN_x layer to 7.72 A (Fig. 4b) for the module based on the non-SiN_x Si cell by losses of the passivation and AR effects. The η slightly decreased from 14.6% to 14.0% with decreasing fill factor from 0.74 to 0.72 after the PID test, although the η of the standard module based on the FJ Si cell with the SiN_x layer decreased from 17.5% to 14.6% (the power output decreased by about 17%) after the same PID test, as shown in Fig. 2a. No change was observed in the EL image for the module based on non-SiN_x cell after the PID test (Fig. 4b); the EL image before the PID test is darker than that for the standard FJ Si PV module with the SiN_x layer (Fig. 3). These results indicate that remarkable degradation observed in the standard FJ Si PV module due to the surface polarization did not occur in the module based on the non-SiN_x Si cell.

Fig. 5 shows spectra of EQE for the modules based on the standard

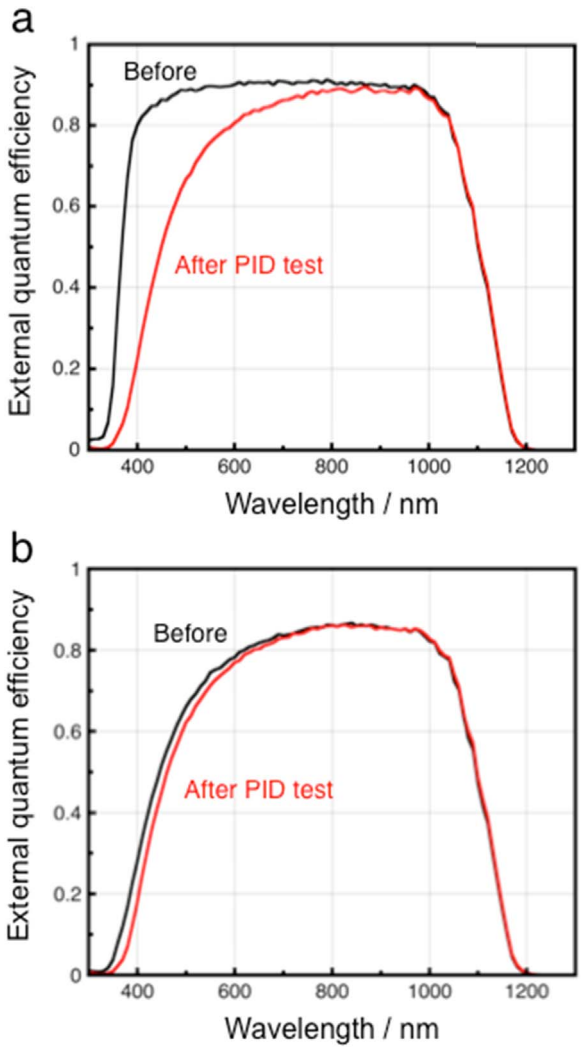

Fig. 5. Spectra of external quantum efficiency for the standard n-type FJ Si PV modules; (a) with and (b) without the SiN_x layer before (black line) and after (red line) PID tests by applying −100 V at 60 °C for 1 h. (For interpretation of the references to color in this figure legend, the reader is referred to the web version of this article.)

n-type FJ Si solar cells (a) with and (b) without the SiN_x layer before and after the PID tests by applying −100 V at 60 °C for 1 h. As shown in Fig. 5a, the EQE in the range from 400 to 600 nm for the standard FJ Si module having the SiN_x layer significantly decreased after the PID test, although no change was observed in the range from 800 to 1100 nm, as reported in the previous paper [27]. Sharma and co-workers reported that when the value of front surface recombination velocity increases, the spectral response of crystalline Si PV cell decreases in the short-wavelength region (e.g. $\lambda < 500$ nm) [32]. Because of the high absorption coefficient of Si for photons of short-wavelength region, such as $\lambda < 500$ nm, the most of the incident photons are absorbed in the heavily doped front emitter region of the cell [32]. Therefore, we consider that the change in the spectrum of EQE for the standard module shown in Fig. 5a is caused by the enhanced front surface recombination.

In contrast, the spectrum of EQE for the n-type FJ Si PV module based on the non-SiN_x cell did not so change after the PID test (Fig. 5b). Additionally, the EQE spectrum for the standard module including the SiN_x layer after the PID test (Fig. 5a) is very similar to that for the module based on the non-SiN_x cell (Fig. 5b). These results suggest that PID in n-type Si PV modules can be approximately explained by a loss of passivation effect by the SiN_x layer.

3.3. TR-DRS measurement

Fig. 6 shows normalized transient absorption kinetics of the standard n-type FJ Si PV module (with a SiN_x layer) probed at 1500–1800 nm by excitation of 400 nm (red line), 532 nm (blue line), and 1064 nm (black line); (a) non-PID and (b) after PID occurred by applying −1000 V at 85 °C for 2 h. The absorption observed after excitation is attributed to electrons in the conduction band (or holes in the valence band), and the decay profile indicates charge recombination process. As shown in Fig. 6a, the transient absorption kinetics showed similar decay profiles (time constant, τ=~30 μs) without excitation-wavelength dependence in the standard FJ Si PV module (non-PID sample). On the other hand, faster decay profiles (τ=~400 ns) were observed by excitation at 400 nm and 532 nm after PID occurred, although the decay profile by excitation at 1064 nm did not change after PID (Fig. 6b). These results directly indicate that surface charge recombination was enhanced by PID in the standard FJ Si PV module.

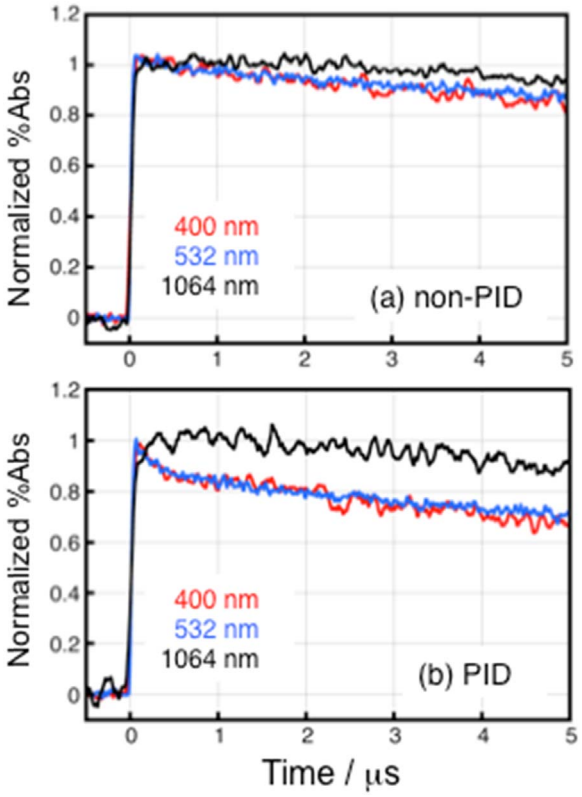

Fig. 6. Transient absorption kinetics of n-type FJ Si PV modules probed at > 1500 nm by excitation of 400 nm (red line), 532 nm (blue line), and 1064 nm (black line); (a) non-PID and (b) after PID occurred by applying −1000 V at 85 °C for 2 h. (For interpretation of the references to color in this figure legend, the reader is referred to the web version of this article.)

Faster decay profiles (τ=~400 ns) by excitation at 400 nm and 532 nm were also observed in the Si PV module based on the non-SiN_x Si cell after a PID test (−100 V at 60 °C for 1 h), whose EQE spectrum (Fig. 5b) was similar to that for the standard FJ Si PV module with the SiN_x layer after PID (Fig. 5a), as mentioned in Section 3.2. This result also implies that the faster decay profiles are related to the lower EQE performance in the short-wavelength region, and PID in n-type Si PV modules approximately corresponds to a loss of passivation effect by the SiN_x layer, enhancing surface charge recombination.

3.4. PID in commercial PV modules

In order to estimate the property of commercial n-type Si PV modules against PID, we chose three commercial modules, module A with an HJ Si solar cell, modules B and C with interdigitated BC Si cells (the PV supplier is different). Firstly, positive voltage (+1000 V) was applied to the Si cell with respect to the Al frame of the module at 85 °C with relative humidity of 85% for 96 h in an environmental chamber, and then secondary test was carried out by applying negative voltage (−600 V or −1000 V) at 85 °C with 85% for 96 h, as mentioned in Experimental section. For example, no degradation was observed in the module A based on the HJ Si cell by applying both +1000 V for 96 h and −1000 V for 96 h at 85 °C with 85% humidity (Fig. 7a), indicating its high PID-resistance property. Generally, HJ Si solar cells have a layer of transparent conducting oxide (TCO) on the top for carrier collection. The TCO layer is considered to effectively suppress the surface polarization on the surface due to its high conductivity (see Section 3.6).

In contrast to the module A, the power output of the module B with a BC Si cell decreased by about 20% after the PID test by applying +1000 V at 85 °C with 85% for 96 h (Fig. 7b). After the secondary test by applying −1000 V at 85 °C with 85% for 96 h, the performance was partially recovered. In the case of the module C with another BC Si cell, the power output decreased by about 6% after the PID test by applying −600 V at 85 °C with 85% for 96 h (we could not apply −1000 V because leakage current during the test was over 1 mA, which is the system limit of the power supply), whereas no degradation was observed by applying +1000 V at 85 °C with 85% for 96 h (Fig. 7c). Thus, the PID-resistant property of commercial n-type Si PV modules is remarkably different. As mentioned in Introduction, the voltage polarity leading to PID would depend on the type of surface layer (n or p) of BC Si solar cells [24–26]. The different voltage polarity causing PID in the modules B and C would be attributed to the different surface layer (n or p) of two BC Si solar cells.

3.5. Mechanism of PID in n-type Si PV modules

Basically, PID in n-type Si PV modules can be explained by the surface polarization effect enhancing surface charge recombination [24–27]. Our results suggest that the surface polarization approximately degrades the passivation effect by the SiN_x layer, resulting in enhanced surface charge recombination, as shown in Figs. 5 and 6. In addition, other factors might be also related to PID in n-type Si PV modules. For instance, Halm et al. suggested that other effects, e.g. contamination of the emitter by mobile ions, which would result in a degradation of the diffusion length in the emitter, is related to the power drop of an n-type BC solar cell by PID, in addition to

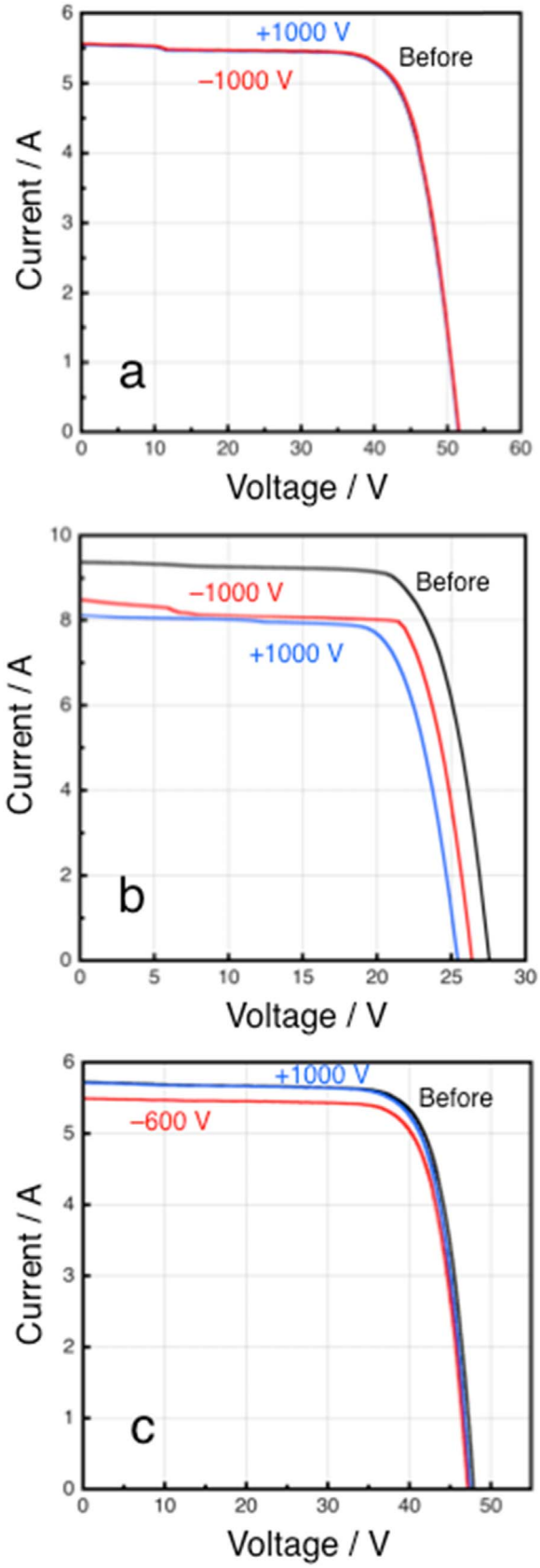

Fig. 7. I-V curves for full-size commercial n-type Si PV modules; (a) module A with an HJ cell, (b) module B with a BC cell, and (c) module C with a BC cell before and after PID tests by applying +1000 V for 96 h and then −1000 V (or −600 V for the module C) for 96 h at 85 °C with 85% relative humidity.

degradation of the front surface passivation enhancing surface charge recombination [26]. Further detail investigation is necessary.

Fig. 8 shows schematic diagrams demonstrating PID in n-type Si PV modules; (a) an n-type BC Si cell whose top is n-layer [24] and (b) the n-type FJ Si cell whose top is p-layer used in this work. Swanson et al. reported that PID in an n-type BC Si PV module whose top is n-layer was observed by applying high positive voltage to the Si cell with respect to the ground, although negative voltage did not result in PID [24]. Negative charge due to leakage current trapped in the SiN_x layer, leading to increasing the concentration of the minority carrier (hole) at the front of n-layer, and consequently increasing surface charge recombination rate [24], as shown in Fig. 8a. The commercial module B with an n-type BC Si cell used in this study (Fig. 7b) might correspond to this case.

PID in the n-type FJ Si PV cell whose p-layer is on the top was observed by applying negative voltage to the Si cell with respect to the Al plate in our experiment. In this case, positive charge due to leakage current would be trapped in the SiN_x layer, leading to increasing the concentration of the minority carrier in p-layer (electron), and consequently increasing charge recombination rate at the surface (Fig. 8b). In the case of n-type BC Si solar cells, which has a p-layer on the surface (p^+ front emitter), PID occurs when negative voltage is applied to the Si cell [26]. In this study, PID was observed by applying negative voltage in the commercial module C based on an n-type BC Si solar cell (Fig. 7c), while the detail surface structure of the Si cell is unclear. These cases can be explained by the degradation mechanism shown in Fig. 8b. Thus, the polarity of voltage causing PID would mainly depend on the type of surface layer (n or p) of n-type Si solar cells.

In this work, the power output reduction of up to 17% was observed in the n-type FJ Si PV module by applying negative voltage to the Si cell with respect to the Al plate (Fig. 2a). The amount of charge trapped at the Si surface would increase with increasing leakage current and time of applying voltage. We can roughly estimate a charge density as 1×10^{13} cm^{-2} from the leakage current and the PID test time for the n-type FJ Si PV module used in this study. Swanson et al. reported that the charge density of 1×10^{12} cm^{-2} causes PID in an n-type BC Si PV module, whereas the power output of the module decreased more than 30% after PID occurred (in this case, not only I_{sc} and V_{oc}, but also fill factor decreased) [24]. On the other hand, the output reduction for the commercial module B with another n-type BC Si PV solar cell was ca. 20%, as shown in Fig. 7b. Thus, the rate of output reduction causing PID in n-type Si PV modules is not consistent.

At the present, we cannot clearly explain why PID did not occur in the n-type RJ Si PV module used in this study (Fig. 2b). The front surface of the n-type RJ Si solar cell is n-layer, which is similar to that of the n-type BC Si solar cell shown in Fig. 8a. Therefore, we can expect that PID due to the surface polarization should occur in the n-type RJ Si PV module by applying positive voltage. However, no degradation was observed in the n-type RJ Si PV module by applying +1000 V at 85 °C for 10 min, as shown in Fig. 2b. It is considered that charges are hard to be trapped at the surface of the n-type RJ Si solar cell used in this study, which would depend on the structure of AR and passivation layers with SiN_x, SiO_x, or other materials, although the detail is unclear. Thus, front surface structures of Si cells, which do not trap charges, might be one of promising techniques for suppression of the surface polarization, resulting in PID in n-type Si PV modules.

3.6. PID- resistant technique for n-type Si PV modules

As shown in Fig. 7a, the commercial module A based on an HJ Si solar cell indicated high PID-resistance property against both negative and positive high voltages. Generally, HJ Si cells have a layer of TCO on the top of cell for carrier collection. High-conductive TCO layers would be able to decrease the influence of charge trapped at the Si surface, and consequently suppress PID in n-type Si PV modules. For instance, we have reported that a $Cu(In,Ga)Se_2$ (CIGS) PV module, which has a

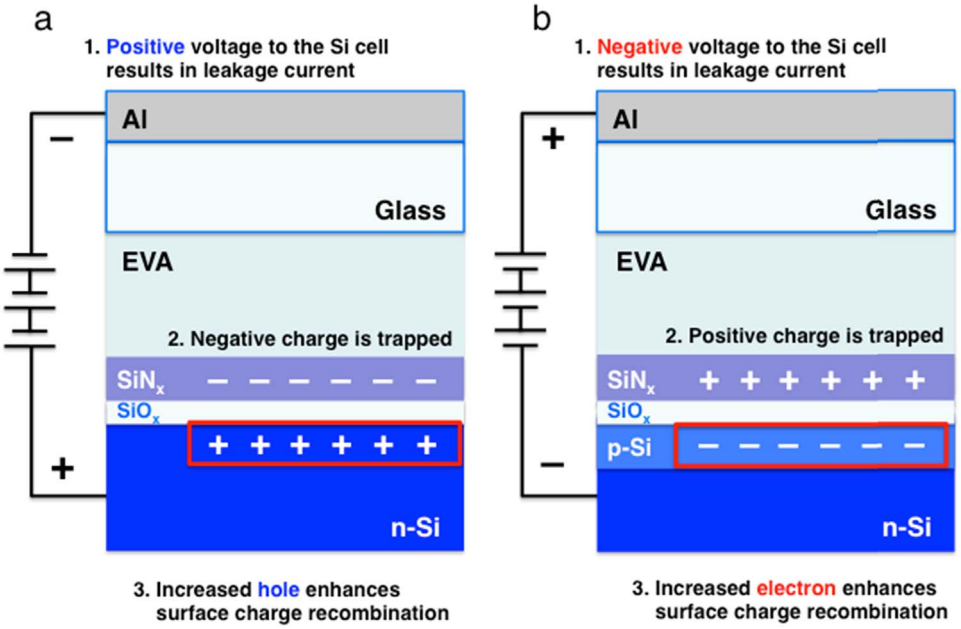

Fig. 8. Schematic diagrams demonstrating the proposed mechanism of PID in n-type Si PV modules; (a) a BC Si solar cell [24] and (b) the FJ Si solar cell used in this work.

ZnO thin layer on the top as the TCO electrode and n-type layer, showed a high PID-resistance property compared to crystalline Si PV modules [33]. A CIGS PV module maintained almost 100% power output after a PID test (−1000 V at 85 °C for 2 h), although the output for p-type multi-crystalline Si PV modules decreased to 5–40% by the same PID test [33]. This high PID-resistivity would be derived from the high conductive ZnO layer, whereas further detail investigation is necessary. An increase in the Si content of SiN_x layers as the AR coating, which increases the conductivity of the layer, is effective to suppress PID in p-type Si PV modules [1,6,19,20]. However, our result obviously indicates that a control of the RI of a SiN_x layer is not effective to prevent the surface polarization causing PID in n-type Si PV modules, as shown in Fig. 4a and mentioned in Section 3.2.

It has been reported that encapsulant, such as ionomer (IO), whose volume resistivity is higher than that of EVA significantly prevents PID in p-type Si PV modules [34–36]. We have reported that an IO encapsulant significantly suppresses PID in an n-type FJ Si PV module [27]. No degradation was observed in a module involving the IO encapsulant instead of conventional EVA encapsulant by applying −1000 V at 85 °C for 2 weeks [27]. Halm et al. also reported that encapsulation materials, which have high volume resistivity, have PID-resistivity for an n-type BC solar cell [26]. Additionally, PID also did not occur in a PV module based on a high-resistivity cover glass, which does not include alkali metals, instead of the conventional soda lime glass by applying −1000 V at 85 °C for 1 week, although the conventional EVA encapsulant was employed (data are not shown). These results imply that high-volume resistivity encapsulants or front cover glasses are also significantly effective to suppress PID in n-type Si PV modules, in addition to high-conductive layers on the top of Si cell.

We have reported that a combined encapsulant composed of the conventional EVA and a thin polyethylene (PE) film (30 μm-thickness) whose volume resistivity is higher than that of EVA remarkably suppresses PID when it was introduced into a p-type crystalline Si PV module [22]. This suppression effect would be attributed to prevention of the electro-migration of Na^+ from the front cover glass to the Si cell because of higher volume resistivity of the PE film. In the n-type FJ Si PV module, however, PID cannot be perfectly prevented by using the combined encapsulant of the EVA and the thin PE film, whereas increasing thickness of the PE film was effective to suppress PID. This suggests that higher volume resistivity of the encapsulant is necessary in order to perfectly suppress PID in n-type Si PV modules than p-type Si PV modules.

4. Conclusions

The power output of the n-type FJ Si PV module decreased by up to 17% after the PID tests of −1000 V at 85 °C for 10 min or −100 V at 60 °C for 1 h, although no degradation was observed in the n-type RJ Si PV module. The decreased performance was completely recovered after applying +1000 V at 85 °C for 10 min. The spectra of EQE and decay profiles of the carriers measured by TR-DRS before and after PID tests indicated that PID in n-type Si PV modules can be basically explained by the surface polarization effect enhancing surface charge recombination between electron and hole on the Si cell. The surface polarization would approximately degrade the passivation effect by SiN_x layers, resulting in the enhanced surface charge recombination. We can approximately estimate the saturated charge density as 1×10^{13} cm^{-2} from the leakage current and the PID test time for the n-type FJ Si solar cell used in this study. The polarity of voltage causing PID in n-type Si PV modules would depend on the type of surface layer (n or p) of Si cells. No PID was observed in the commercial PV module based on an HJ Si cell by applying both positive and negative voltages, whereas PID occurred in commercial PV modules with n-type BC Si solar cells. This suggests that high conductive layers (such as TCO) on the top of Si cell are significantly effective to suppress PID in n-type Si PV modules, in addition to high-volume-resistivity encapsulants (such as IO) or front cover glasses.

Acknowledgments

We thank Dr. S. Kawai in Industrial Technology Center of SAGA and Dr. T. Ishii in Central Research Institute of Electric Power Industry for their support in experiments. We also acknowledge Dr. A. Furube in Tokushima University, Mr. S. Yamaguchi, and Prof. K. Ohdaira in Japan Advanced Institute of Science and Technology for their helpful discussion.

References

[1] S. Pingel, O. Frank, M. Winkler, S. Daryan, T. Geipel, H. Hoehne, J. Berghold, Potential induced degradation of solar cells and panels, in: Proceedings of the 35th IEEE Photovoltaic Specialists Conference (IEEE PVSC), Honolulu, HI, USA, 2010,

pp. 2817–2822.
[2] P. Hacke, M. Kempe, K. Terwilliger, S. Glick, N. Call, S. Johnston, S. Kurtz, I. Bennett, M. Kloos, Characterization of multicrystalline silicon modules with system bias voltage applied in damp heat, in: Proceedings of the 25th European Photovoltaic Solar Energy Conference and Exhibition (EU PVSEC) and 5th World Conference on Photovoltaic Energy Conversion (WCPEC), Valencia, Spain, 2010, pp. 3760–3765.
[3] P. Hacke, K. Terwilliger, R. Smith, S. Glick, J. Pankow, M. Kempe, S. Kurtz, I. Bennett, M. Kroos, System voltage potential-induced degradation mechanisms in PV modules and methods for test, in: Proceedings of the 37th IEEE PVSC, Seattle, WA, USA, 2011, pp. 814–820.
[4] P. Saint-Cast, H. Nagel, D. Wagenmann, J. Schön, P. Schmitt, C. Reichel, S.W. Glunz, M. Hofmann, J. Rentsch, R. Preu, Potential-induced degradation on cell level: the inversion model, in: Proceedings of the 28th EU PVSEC, Paris, France, 2013, pp. 789–792.
[5] M. Schütze, M. Junghänel, O. Friedrichs, R. Wichtendahl, M. Scherff, J. Müller, P. Wawer, Investigations of potential induced degradation of silicon photovoltaic modules, in: Proceedings of the 26th EU PVSEC, Hamburg, Germany, 2011, pp. 3097–3102.
[6] H. Nagel, A. Metz, K. Wangemann, Crystalline Si solar cells and modules featuring excellent stability against potential-induced degradation, in: Proceedings of the 26th EU PVSEC, Hamburg, Germany, 2011, pp. 3107–3112.
[7] A. Raykov, H. Hahn, K.-.H. Stegemann, M. Kutzer, O. Storbeck, H. Neuhaus, W. Bergholz, Towards a root cause model for potential-induced degradation in crystalline silicon photovoltaic cells and modules, in: Proceedings of the 28th EU PVSEC, Paris, France, 2013, pp. 2998–3002.
[8] M. Martin, R. Krause, H. Eckert, M. Pfeifer, D. Kohake, Investigation of potential induced degradation for various module manufactures and technologies, in: Proceedings of the 27th EU PVSEC, Frankfurt, Germany, 2012, pp. 3394–3398.
[9] J. Bauer, V. Naumann, S. Großer, C. Hagendorf, M. Schütze, O. Breitenstein, On the mechanism of potential-induced degradation in crystalline silicon solar cells, Phys. Status Solidi RRL 6 (2012) 331–333.
[10] V. Naumann, C. Hagendorf, S. Grosser, M. Werner, J. Bagdahn, Micro structural root cause analysis of potential induced degradation in c-Si solar cells, Energy Procedia 27 (2012) 1–6.
[11] V. Naumann, D. Lausch, S. Großer, M. Werner, S. Swatek, C. Hagendorf, J. Bagdahn, Microstructural analysis of crystal defects leading to potential-induced degradation (PID) of Si solar cells, Energy Procedia 33 (2013) 76–83.
[12] V. Naumann, D. Lausch, A. Graff, M. Werner, S. Swatek, J. Bauer, A. Hähnel, O. Breitenstein, S. Großer, J. Bagdahn, C. Hagendorf, The role of stacking faults for the formation of shunts during potential-induced degradation of crystalline Si solar cells, Phys. Status Solidi RRL 7 (2013) 315–318.
[13] D. Lausch, V. Naumann, O. Breitenstein, J. Bauer, A. Graff, J. Bagdahn, C. Hagendorf, Potential-induced degradation (PID): introduction of a novel test approach and explanation of increased depletion region recombination, IEEE J. Photovolt. 4 (2014) 834–840.
[14] V. Naumann, D. Lausch, A. Hähnel, J. Bauer, O. Breitenstein, A. Graff, M. Werner, S. Swatek, S. Großer, J. Bagdahn, C. Hagendorf, Explanation of potential-induced degradation of the shunting type by Na decoration of stacking faults in Si solar cells, Sol. Energy Mater. Sol. Cells 120 (2014) 383–389.
[15] V. Naumann, D. Lausch, C. Hagendorf, Sodium decoration of PID-s crystal defects after corona induced degradation of bare silicon solar cells, Energy Procedia 77 (2015) 397–401.
[16] H.-C. Liu, C.-T. Huang, W.-K. Lee, M.-H. Lin, High voltage stress impact on p type crystalline silicon PV module, Energy Power Eng. 5 (2013) 455–458.
[17] S. Hoffmann, M. Koehl, Effect of humidity and temperature on the potential-induced degradation, Prog. Photovolt.: Res. Appl. 22 (2014) 173–179.
[18] M. Kambe, K. Hara, K. Mitarai, S. Takeda, M. Fukawa, N. Ishimaru, M. Kondo, PID-free c-Si PV module using aluminosilicate chemically strengthened glass, in: Proceedings of the 28th EU PVSEC, Paris, France, 2013, pp. 2861–2864.
[19] K. Mishina, A. Ogishi, K. Ueno, T. Doi, K. Hara, N. Ikeno, D. Imai, T. Saruwatari, M. Shinohara, T. Yamazaki, A. Ogura, Y. Ohshita, A. Masuda, Investigation on antireflection coating for high resistance to potential-induced degradation, Jpn. J. Appl. Phys. 53 (2014) (03CE01-1–03CE01-4).
[20] K. Mishina, A. Ogishi, K. Ueno, S. Jonai, N. Ikeno, T. Saruwatari, K. Hara, A. Ogura, T. Yamazaki, T. Doi, M. Shinohara, A. Masuda, Plasma-enhanced chemical-vapor deposition of silicon nitride film for high resistance to potential-induced degradation, Jpn. J. Appl. Phys. 54 (2015) (08KD12-1–08KD12-6).
[21] K. Hara, H. Ichinose, T.N. Murakami, A. Masuda, Crystalline Si photovoltaic modules based on TiO_2-coated cover glass against potential-induced degradation, RSC Adv. 4 (2014) 44291–44295.
[22] K. Hara, S. Jonai, A. Masuda, Crystalline Si photovoltaic modules functionalized by a thin polyethylene film against potential and damp-heat-induced degradation, RSC Adv. 5 (2015) 15017–15023.
[23] S. Jonai, K. Hara, Y. Tsutsui, H. Nakahama, A. Masuda, Relationship between cross-linking conditions of ethylene vinyl acetate and potential induced degradation for crystalline silicon photovoltaic modules, Jpn. J. Appl. Phys. 54 (2015) (08KG01-1–08KG01-5).
[24] R. Swanson, M. Cudzinovic, D. DeCeuster, V. Desai, J. Jürgens, N. Kaminar, W. Mulligan, L. Rodrigues-Barbosa, D. Rose, D. Smith, A. Terao, K. Wilson, The surface polarization effect in high-efficiency silicon solar cells, in: Technical Digests of the 15th International Photovoltaic Science & Engineering Conference (PVSEC-15), Shanghai, China, 2005, pp. 410–411.
[25] V. Naumann, T. Geppert, S. Großer, D. Wichmann, H.-J. Krokoszinski, M. Werner, C. Hagendorf, Potential-induced degradation at interdigitated back contact solar cells, Energy Procedia 55 (2014) 498–503.
[26] A. Halm, A. Schneider, V.D. Mihailetchi, L.J. Koduvelikulathu, L.M. Popescu, G. Galbiati, H. Chu, R. Kopecek, Potential-induced degradation for encapsulated n-type IBC solar cells with front floating emitter, Energy Procedia 77 (2015) 356–363.
[27] K. Hara, S. Jonai, A. Masuda, Potential-induced degradation in photovoltaic modules based on n-type single crystalline Si solar cells, Sol. Energy Mater. Sol. Cells 140 (2015) 361–365.
[28] T. Asahi, A. Furube, H. Fukumura, M. Ichikawa, H. Masuhara, Development of a femtosecond diffuse reflectance spectroscopic system, evaluation of its temporal resolution, and applications to organic powder systems, Rev. Sci. Instrum. 69 (1998) 361–371.
[29] A. Furube, T. Asahi, H. Masuhara, H. Yamashita, M. Anpo, Charge carrier dynamics of standard TiO_2 catalysts revealed by femtosecond diffuse reflectance spectroscopy, J. Phys. Chem. B 103 (1999) 3120–3127.
[30] S. Yamaguchi, A. Masuda, K. Ohdaira, Changes in the current density–voltage and external quantum efficiency characteristics of n-type single-crystalline silicon photovoltaic modules with a rear-side emitter undergoing potential-induced degradation, Sol. Energy Mater. Sol. Cells 151 (2016) 113–119.
[31] S. Pingel, S. Janke, O. Frank, Recovery methods for modules affected by potential induced degradation (PID), in: Proceedings of the 27th EU PVSEC, Frankfurt, Germany, 2012, pp. 3379–3383.
[32] A.K. Sharma, S.K. Agarwal, S.N. Singh, Determination of front surface recombination velocity of silicon solar cells using the short-wavelength spectral response, Sol. Energy Mater. Sol. Cells 91 (2007) 1515–1520.
[33] S. Yamaguchi, S. Jonai, K. Hara, H. Komaki, Y. Shimizu-Kamikawa, H. Shibata, S. Niki, Y. Kawakami, A. Masuda, Potential-induced degradation of Cu(In,Ga)Se2 photovoltaic modules, Jpn. J. Appl. Phys. 54 (2015) (08KC13-1–08KC13-7).
[34] J. Kapur, A. Bennett, J. Norwood, B. Hamzavytehrany, I. Kueppenbender, Tailoring ionomer encapsulants as low cost solution to potential induced degradation, in: Proceedings of the 28th EU PVSEC, Paris, France, 2013, pp. 476–479.
[35] S.-.H. Schulze, A. Apel, R. Meitzner, M. Schak, C. Ehrich, J. Schneider, Influence of polymer properties on potential induced degradation of PV-modules, in: Proceedings of the 28th EU PVSEC, Paris, France, 2013, pp. 503–507.
[36] C.G. Reid, S.A. Ferrigan, J.I.F. Martinez, J.T. Woods, Contribution of PV encapsulant composition to reduction of potential induced degradation (PID) of crystalline silicon PV cells, in: Proceedings of the 28th EU PVSEC, Paris, France, 2013, pp. 3340–3346.